ELSEVIER

Inorganica Chimica Acta 225 (1994) 137–144

Inorganica Chimica Acta

Electrochemical recognition of Group 1 and 2 metal cations by redox-active ionophores

Paul D. Beer[a,*], Zheng Chen[a], Michael G.B. Drew[b], Alexandra J. Pilgrim[a]

[a]*Inorganic Chemistry Laboratory, University of Oxford, South Parks Road, Oxford OX1 3QR, UK*
[b]*Department of Chemistry, University of Reading, Whiteknights, PO Box 224, Reading RG6 2AD, UK*

Received 15 March 1994

Abstract

New ferrocene bis(aza-crown ethers) **6** and **7** have been synthesised in which a ferrocene redox centre bridges the two aza-crown ether moieties, linked via methylene covalent bonds. Coordination chemical investigations revealed both ligands to form complexes with sodium, potassium, magnesium and barium cations. Single crystal X-ray structures of **4** and the $[\mathbf{6}\cdot 2K^+](PF_6^-)_2$ complex have also been determined. Electrochemical investigations have demonstrated that the binding of Na^+, K^+, Mg^{2+} and Ba^{2+} guest cations by **6** and **7** results in shifts of the respective ferrocene–ferrocenium redox couple to more positive potentials. The magnitude of these one-wave anodic shifts is related to the charge:radius ratio of the cationic guest species. Electrochemical recognition competition experiments suggest **6** exhibits a degree of selectivity for the Ba^{2+} cation.

Keywords: Electrochemistry; Crystal structures; Ferrocene complexes; Crown ether complexes

---

1. Introduction

The prospect of advancing chemical sensor technology, modelling electron transfer processes in biological systems and producing new redox catalysts has led to considerable interest in the design and syntheses of redox-active macrocyclic receptor molecules that contain a redox centre in close proximity to a host binding site [1]. We and others have demonstrated that reducible [2–5] or oxidisable [6–14] redox-active macrocycles can electrochemically recognise cationic (metal, ammonium [15]) and anionic (halides, nitrate, phosphate, hydrogen sulfate) [16,17] guest species in polar organic solvents and in some cases water [18]. A combination of many factors including (i) redox-active host–guest complimentarity, (ii) the polarising power of the guest, (iii) proximity of the host binding site to the redox centre, and (iv) nature of the bond linkage from the host binding site to the redox centre can contribute to the experimentally observed magnitude and type (one or two waves) of the electrochemical perturbation in the respective redox couples of these host systems produced by charged guest binding. Focussing on the latter two factors we report here the synthesis, coordination and electrochemistry of new ferrocene bis aza-crown ethers in which a methylene unit links the aza-crown ether recognition site to the ferrocene redox-active centre. In addition, a single crystal X-ray structure of a bis-potassium complex of one redox-active ionophore is described. A preliminary report of this work has been published [19].

2. Experimental

NMR spectra were measured using a Bruker AM300 spectrometer at 300 MHz for ^1H and 75.45 MHz for ^{13}C. Elemental analyses were performed by the micro analytical service at the Inorganic Chemistry Laboratory of the University of Oxford. IR spectra were measured using a Mattson Polaris FT spectrophotometer model IR 10410E. Spectra were recorded from 4000–600 cm^{-1} as KBr discs or between NaCl plates (for oils). UV and Vis absorption spectra were recorded on a Perkin-Elmer Lambda 6 UV–Vis spectrophotometer.

FAB mass spectrometry was undertaken by the SERC mass spectrometry service at University College, Swansea. Cyclic voltammetric studies were performed on a Princeton Applied Research potentiostat/galvanostat model 273. Reference electrode and acquisition pa-

---

*Corresponding author.

SSDI 0020-1693(94)04040-3

rameters are quoted in individual cases. Melting points were recorded in open glass capillary tubes on a Gallenkamp melting point apparatus and are uncorrected. Where necessary, solvents were distilled prior to use. The following drying agents were used before distillation under nitrogen: acetonitrile, dichloromethane and TMEDA were distilled from CaH_2; toluene and THF were distilled from sodium, the latter using benzophenone as an indicator. Hexane and pentane were dried over sodium wire; triethylamine was distilled from and stored over potassium hydroxide pellets. 1,1′-Bis(chlorocarbonyl)ferrocene (**1**) [20], aza-18-crown-6 (**2**) [21] and aza-15-crown-5 (**3**) [21] were prepared using literature procedures. Unless stated otherwise, commercial grade reagents were used without further purification.

2.1. Syntheses

2.1.1. Ferrocene bis(carbonyl aza-18-crown-6) (4)

A solution of 1,1′-bis(chlorocarbonyl) ferrocene (0.242 g, 0.78 mmol) in dry toluene (75 ml) was added dropwise over 30 min to a stirred solution of aza-18-crown-6 (0.42 g, 1.59 mmol) and triethylamine (0.223 ml, 1.60 mmol) in dry toluene (75 ml) under nitrogen. The reaction mixture was then stirred for 1 h before being filtered and evaporated under reduced pressure. The residue was dissolved in CH_2Cl_2 (75 ml), washed with water (3×75 ml), dried ($MgSO_4$) and the solvent removed before being chromatographed on an alumina column using first CH_2Cl_2 then CH_2Cl_2/methanol (98:2, vol./vol.) as eluant. The product, an orange oil, was recrystallised from diethyl ether and hexane to give orange crystals in 82% yield (0.49 g). M.p. = 65–67 °C. IR data (KBr disc): 3077, 1615, 2780 cm^{-1}. ^1H NMR ($CDCl_3$, 300 MHz) δ: 3.65–3.72 (m, 48H, N–CH_2 and CH_2–O), 4.37 (t, $J=1.9$ Hz, 4H, Cp–H), 4.69 (t, $J=1.9$ Hz, Cp–H). ^{13}C NMR ($CDCl_3$, 75.42 MHz) δ: 70.56, 70.70, 70.64 (CH_2–O), 71.79, 71.95 (Cp), 80.08 (*ipso* Cp), 169.95 (CON). *Anal.* Found: C, 56.73; H, 7.48; N, 3.60. Calc. for $C_{36}H_{56}O_{12}N_2Fe$: C, 56.54; H, 7.38; N, 3.66%.

2.2.2. Ferrocene bis(carbonyl aza-15-crown-5) (5)

An analogous synthetic procedure to the preparation of **4** was employed using 1,1′-bis(chlorocarbonyl) ferrocene (**1**) (0.25 g, 0.80 mmol), aza-15-crown-5 (**3**) (0.35 g, 1.60 mmol) and triethylamine (0.22 ml, 1.60 mmol). An orange semi-solid was isolated in 78% yield (0.42 g). ^1H NMR ($CDCl_3$, 300 MHz) δ: 3.60–3.80 (m, 40H, N-CH_2 and CH_2–O), 4.37 (t, $J=1.9$ Hz, 4H, Cp–H), 4.71 (t, $J=1.9$ Hz, 4H, Cp–H). ^{13}C NMR ($CDCl_3$, 75.42 MHz) δ: 69.27, 70.20, 70.28 (CH_2–O), 71.85, 71.98 (Cp), 79.43 (*ipso* Cp), 167.03 (CON). *Anal.* Found: C, 54.85; H, 7.36; N, 3.99. Calc. for $C_{32}H_{48}O_8N_2Fe \cdot H_2O$: C, 55.33; H, 7.26; N 4.03%.

2.2.3. Ferrocene bis(methylene aza-18-crown-6) (6)

Ferrocene bis(carbonyl aza-18-crown-6) (**4**) (0.15 g, 0.20 mmol) was dissolved in dry CH_2Cl_2 (10 ml) containing dry THF (2 ml) under N_2 and to this stirred solution and ambient temperature was added an eightfold excess of $LiAlH_4$ (60 mg, 1.58 mmol). The reaction was stirred for 30 min before being diluted with CH_2Cl_2 (10 ml) and quenched with an aqueous, saturated solution of sodium tartrate (10 ml). The organic layer was separated and washed with deionised water (3×15 ml), dried over $MgSO_4$ and the solvent removed in vacuo. The residue was purified on a column of alumina (deactivated with 3% H_2O) using firstly CH_2Cl_2 then CH_2Cl_2/methanol (99:1, vol./vol.) as eluant and the product evaporated in vacuo to give a yellow oil in 60% yield (90 mg). IR data (NaCl plates): 3085, 2772, 1451, 1118 cm^{-1}. FAB MS: *m/z* 737 ($M+H^+$), 759 ($M+Na^+$). ^1H NMR ($CDCl_3$, 300 MHz) δ: 2.67 (t, $J=5.6$ Hz, 8H, N–CH_2), 3.53–3.66 (m, 44H, CH_2–O), 4.02–4.06 (m, 8H, Cp–H). ^{13}C NMR ($CDCl_3$, 75.42 MHz) δ: 53.16 (N–CH_2), 54.97 (ferrocene–CH_2–N), 68.53, 70.67, (Cp), 70.37, 69.79, 70.76, 70.85 (CH_2–O), 83.16 (*ipso* Cp). *Anal.* Found: C, 57.76; H, 8.17; N, 3.85. Calc. for $C_{36}H_{60}O_{12}N_2Fe \cdot H_2O$: C, 57.27; H, 8.28; N 3.71%.

2.2.4. Ferrocene bis(methylene aza-15-crown-5) (7)

Compound **5** (0.299 g, 0.46 mmol) was reduced with $LiAlH_4$ (0.14 g, 3.7 mmol) using the same method as for the reduction of (**4**) giving a yellow oil in a yield of 20% (60 mg). FAB-MS: *m/z* 649 ($M+H^+$). ^1H NMR ($CDCl_3$, 300 MHz) δ: 2.69 (t, $J=5.9$ Hz, 8H, N–CH_2), 3.53–3.67 (m, 36H, Fc–CH_2 and CH_2–O), 4.03–4.06 (m, 8H, Cp–H). ^{13}C NMR ($CDCl_3$, 75.42 MHz) δ: 53.46 (N–CH_2), 55.75 (Fc–CH_2–N), 68.69, 70.42 (Cp), 69.69, 70.14, 70.75, 70.95 (CH_2–O), 83.15 (*ipso* Cp).

2.2.5. Isolation of complexes of 6

To a solution of **6** (50 mg, 0.068 mmol) in CH_2Cl_2 (2 ml) was added an excess of the particular metal cation ($K^+PF_6^-$; Na^+, Mg^{2+} or Ba^{2+} as their perchlorates). The resulting suspension was then agitated in an ultrasound bath at 35 °C for 30 min before being diluted with a further 2 ml CH_2Cl_2, filtered and evaporated under reduced pressure. The K^+ and Ba^{2+} complexes were successfully isolated as pale yellow powders in nearly quantitative yields with satisfactory analyses. Isolation of the Na^+ and Mg^{2+} complexes proved unsuccessful.

2.3. Crystallography

2.3.1. Crystal data for 4

$C_{36}H_{56}FeN_2O_{12}$, $M=764.7$, monoclinic, space group $C2/c$, $a=30.543(8)$, $b=8.141(4)$, $c=15.559(7)$ Å, $\beta=111.54(1)°$, $V=3598.4(5)$ Å^3, $Z=4$, $D_c=1.41$ g cm^{-3},

Table 1
Atomic coordinates ($\times 10^4$) with e.s.d.s in parentheses for **4**

Atom	x	y	z
Fe(1)	5000	665(2)	7500
N(1)	5501(3)	−2357(9)	6217(4)
C(2)	5641(3)	−3974(13)	6037(7)
C(3)	5780(4)	−5058(14)	6867(8)
O(4)	6199(3)	−4523(9)	7513(5)
C(5)	6259(4)	−4640(13)	8428(7)
C(6)	6709(4)	−3784(12)	8988(7)
O(7)	6638(2)	−2103(8)	8804(4)
C(8)	7062(3)	−1295(11)	9130(5)
C(9)	7011(3)	378(12)	8765(6)
O(10)	7467(3)	1066(8)	9050(4)
C(11)	7483(5)	2663(13)	8716(8)
C(12)	7579(4)	2679(13)	7846(7)
O(13)	7275(2)	1927(8)	7121(4)
C(14)	6885(4)	2935(12)	6636(7)
C(15)	6520(4)	1939(14)	5972(6)
O(16)	6325(2)	928(8)	6468(4)
C(17)	6023(3)	−268(12)	5944(5)
C(18)	5868(3)	−1180(11)	6616(5)
C(20)	5050(3)	−2137(11)	6120(5)
O(21)	4775(2)	−3298(8)	5889(5)
C(31)	4876(3)	−558(11)	6295(5)
C(32)	4458(3)	−464(11)	6487(5)
C(33)	4353(3)	1200(11)	6564(5)
C(34)	4693(3)	2180(12)	6393(5)
C(35)	5010(3)	1099(1)	6230(5)

Table 2
Selected torsion angles for **4**

C(20)–N(1)–C(2)–C(3)	−86.7(10)
C(18)–N(1)–C(2)–C(3)	84.3(10)
N(1)–C(2)–C(3)–O(4)	70.0(11)
C(2)–C(3)–O(4)–C(5)	143.7(9)
C(3)–O(4)–C(5)–C(6)	−172.5(9)
O(4)–C(5)–C(6)–O(7)	69.0(10)
C(5)–C(6)–O(7)–C(8)	−166.8(7)
C(6)–O(7)–C(8)–C(9)	167.0(7)
O(7)–C(8)–C(9)–O(10)	−173.9(7)
C(8)–C(9)–O(10)–C(11)	177.1(7)
C(9)–O(10)–C(11)–C(12)	−95.9(11)
O(10)–C(11)–C(12)–O(13)	62.9(15)
C(11)–C(12)–O(13)–C(14)	82.8(11)
C(12)–O(13)–C(14)–C(15)	−170.1(8)
O(13)–C(14)–C(15)–O(16)	71.2(10)
C(14)–C(15)–O(16)–C(17)	−170.6(8)
C(15)–O(16)–C(17)–C(18)	179.4(8)
C(20)–N(1)–C(18)–C(17)	−104.6(10)
C(2)–N(1)–C(18)–C(17)	85.0(10)
O(16)–C(17)–C(18)–N(1)	172.0(7)
C(18)–N(1)–C(20)–O(21)	−170.0(9)
C(18)–N(1)–C(20)–C(31)	9.1(12)
N(1)–C(20)–C(31)–C(32)	−159.1(7)
O(21)–C(20)–C(31)–C(35)	−152.2(9)

Table 3
Atomic coordinates ($\times 10^4$) with e.s.d.s in parentheses for $[\mathbf{6}\cdot 2\mathrm{K}^+](\mathrm{PF}_6^-)_2$

Atom	x	y	z
Fe(1)	5000	0	0
C(11)	4128(4)	1407(9)	343(3)
C(12)	4684(6)	2406(12)	98(6)
C(13)	4597(6)	1893(14)	−649(5)
C(14)	4015(5)	641(15)	−757(4)
C(15)	3720(4)	338(12)	−98(4)
C(16)	3994(4)	1469(9)	1207(3)
N(17)	3239(4)	2378(7)	1363(3)
C(18)	2436(4)	1666(11)	1058(4)
C(19)	2275(6)	−20(11)	1315(4)
O(20)	2284(4)	33(6)	2059(3)
C(21)	2088(6)	−1511(11)	2351(5)
C(22)	1974(6)	−1266(12)	3113(5)
O(23)	2731(3)	−639(7)	3485(3)
C(24)	2681(7)	−559(12)	4237(4)
C(25)	3461(8)	273(12)	4588(5)
O(26)	3391(4)	1940(7)	4387(3)
C(27)	4050(6)	2933(13)	4750(5)
C(28)	3917(7)	4603(13)	4476(6)
O(29)	4154(4)	4662(7)	3784(4)
C(30)	4128(8)	6216(13)	3466(7)
C(31)	4393(7)	6104(13)	2751(7)
O(32)	3775(4)	5179(6)	2309(3)
C(33)	3944(7)	5104(12)	1594(6)
C(34)	3283(6)	4106(10)	1156(5)
K(1)	3178(1)	2352(2)	2917(1)
P(1)	5811(1)	959(3)	3057(1)
F(11)	5624(5)	−381(9)	2476(4)
F(12)	5747(6)	−420(12)	3607(4)
F(13)	6773(5)	572(14)	3123(8)
F(14)	4826(5)	1346(13)	2982(6)
F(15)	5850(9)	2262(12)	2456(6)
F(16)	6020(7)	2282(11)	3625(6)

Table 4
Selected torsion angles for $[\mathbf{6}\cdot 2\mathrm{K}^+](\mathrm{PF}_6^-)_2$

C(14)–C(11)–C(16)–N(17)	99.4(9)
C(11)–C(16)–N(17)–C(18)	64.3(8)
C(16)–N(17)–C(18)–N(19)	61.1(8)
N(17)–C(18)–C(19)–O(20)	59.2(9)
C(18)–C(19)–O(20)–C(21)	176.7(7)
C(19)–O(20)–C(21)–C(22)	−170.8(7)
O(20)–C(21)–C(22)–O(23)	−60.1(10)
C(21)–C(22)–O(23)–C(24)	−173.4(8)
C(22)–O(23)–C(24)–C(25)	−174.2(8)
O(23)–C(24)–C(25)–O(26)	70.8(10)
C(24)–C(25)–O(26)–C(27)	173.3(8)
C(25)–O(26)–C(27)–C(28)	178.2(9)
O(26)–C(27)–C(28)–O(29)	−73.8(10)
C(27)–C(28)–O(29)–C(30)	−175.1(8)
C(28)–O(29)–C(30)–C(31)	179.7(8)
O(29)–C(30)–C(31)–O(32)	66.6(11)
C(30)–C(31)–O(32)–C(33)	175.7(8)
C(31)–O(32)–C(33)–C(34)	179.4(8)
C(16)–N(17)–C(34)–C(33)	−68.3(9)
O(32)–C(33)–C(34)–N(17)	−63.2(10)

$\lambda = 0.7197$ Å, $\mu = 4.90$ cm^{-1}, $F(000) = 1632$, $T = 293(2)$ K.

Unit cell parameters and intensity data for a single crystal (0.2×0.2×0.2 mm) were collected with Mo Kα

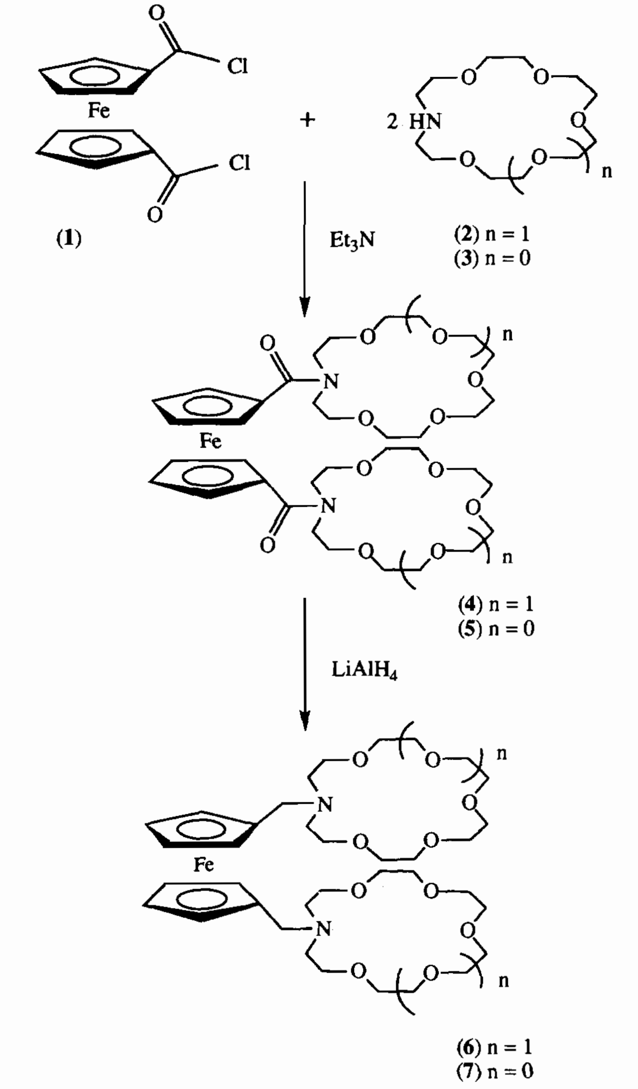

Scheme 1.

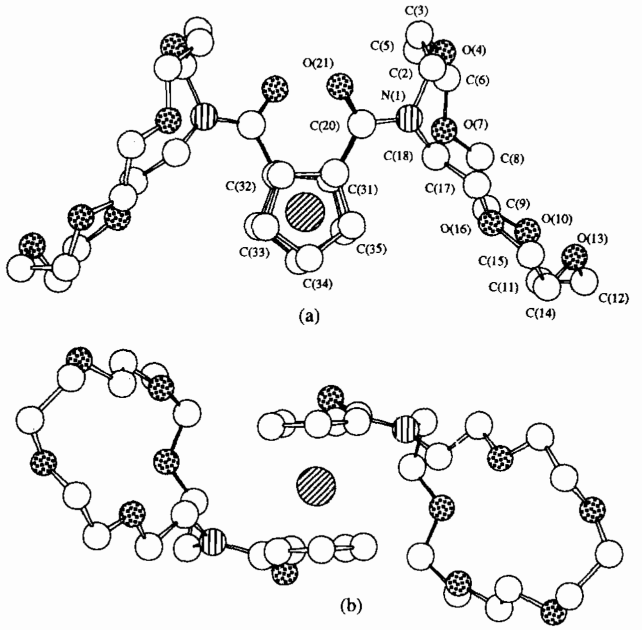

Fig. 1. Crystal structure of **4**: (a) view perpendicular to C_2 axis: (b) view down C_2 axis.

radiation using the MARresearch image plate system. The crystals were positioned at 70 mm from the X-ray source. 120 frames were measured at 2° intervals with a counting time of 5 min. 10 345 reflections ($0 \leqslant h \leqslant 34$, $0 \leqslant k \leqslant 8$, $-17 \leqslant l \leqslant 16$) were measured with a 2θ maximum of 23.91° of which 2243 with $I > 2\sigma(I)$ were independent and used in the subsequent refinement. The structure was refined by full-matrix least-squares on F^2 using anisotropic thermal parameters for non-hydrogen atoms and isotropic thermal parameters for hydrogen atoms. The final R value was 0.0795 (0.0848) and in the final Fourier difference map the maximum and minimum peaks were 0.674 and -0.519 e Å^{-3}. Data analysis was carried out with the XDS program [22] and the structure was solved using direct methods with the SHELX 86 program [23]. The structure was then refined with SHELXL [24]. All calculations were carried out on a Silicon Graphics R4000 workstation at the University of Reading. Crystallographic data for **4** are given in Tables 1 and 2.

2.3.2. Crystal data for [**6**·2K$^+$](PF$_6^-$)$_2$

$C_{36}H_{60}F_{12}FeK_2N_2O_{10}P_2$, $M = 1104.8$, monoclinic, space group $P2_1/a$, $a = 15.789(5)$, $b = 8.094(3)$, $c = 18.651(5)$ Å, $\beta = 96.69(1)$°, $V = 2367.3$ Å^3, $Z = 4$, $D_c = 1.544$ g cm^{-3}, $\lambda = 0.7197$ Å, $\mu = 6.62$ cm^{-1}, $F(000) = 1136$, $T = 293(2)$ K.

Unit cell parameters and intensity data for a single crystal (0.2×0.2×0.02 mm) were collected with Mo Kα radiation using the MARresearch image plate system. The crystals were positioned at 75 mm from the X-ray source. 90 frames were measured at 2° intervals with a counting time of 2 min. 4025 independent reflections ($-18 \leqslant h \leqslant 18$, $0 \leqslant k \leqslant 9$, $-22 \leqslant l \leqslant 22$) were measured with a 2θ maximum of 25.08° of which 2820 with $I > 2\sigma(I)$ were used in the subsequent refinement. The structure was refined by full-matrix least-squares on F^2 using anisotropic thermal parameters for non-hydrogen atoms and isotropic thermal parameters for hydrogen atoms. The final R value was 0.056 (0.1236) and in the final Fourier difference map the maximum and minimum peaks were 0.537 and -0.961 e Å^{-3}. Data analysis was carried out with the XDS program and the structure was solved using direct methods with the SHELX 86 program. The structure was then refined with SHELXL. All calculations were carried out on a Silicon Graphics R4000 workstation at the University of Reading. Crystallographic data for [**6**·2K$^+$](PF$_6^-$)$_2$ are given in Tables 3 and 4.

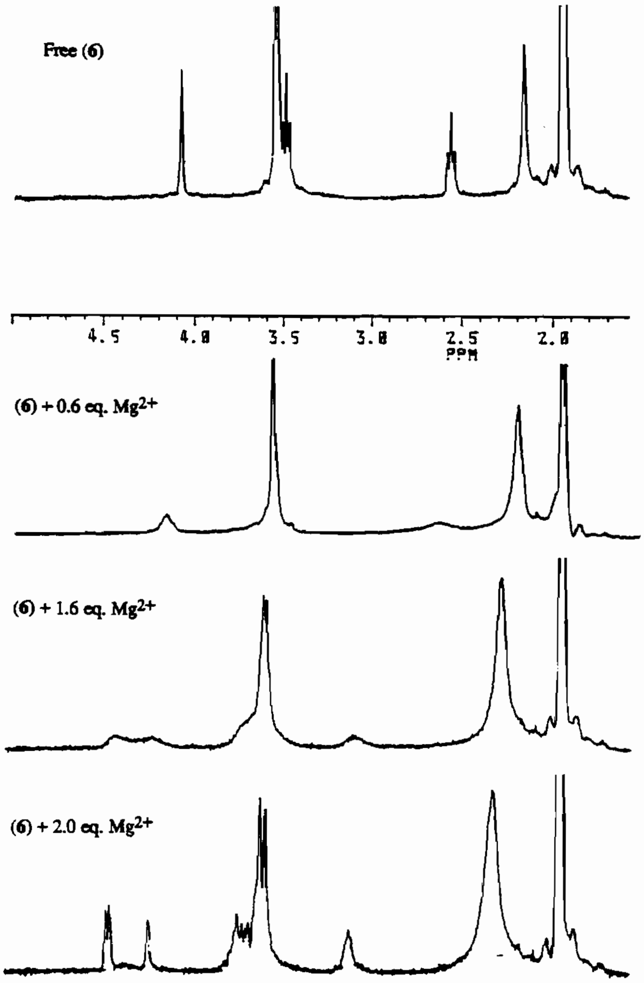

Fig. 2. ^{1}H NMR spectral titration of **6** with Mg^{2+} in CD_3CN.

3. Results and discussion

3.1. Syntheses

The condensation of 1,1′-bis(chlorocarbonyl) ferrocene (**1**) [20] with 2 equiv. of aza-18-crown-6 (**2**) [21] or aza-15-crown-5 (**3**) [21] in the presence of triethylamine gave, after column chromatography, the bis(amide aza-crown ethers) **4** and **5** in 82% and 78% yields, respectively (Scheme 1).

Crystals of **4** suitable for single crystal X-ray structure determination were grown from an ether/hexane solvent mixture. The structure (Fig. 1) has crystallographically imposed C_2 symmetry with the 2-fold axis passing through the iron atom.

The methylene-linked metallocene bis(aza-crown ether) ligands **6** and **7** were prepared via lithium aluminium hydride reduction in a dichloromethane/tetrahydrofuran solvent mixture [18a] (Scheme 1). The structures of these new redox-active ionophores were characterised by elemental analyses, FAB mass spectrometry and ^{1}H and ^{13}C NMR spectroscopy (see Section 2).

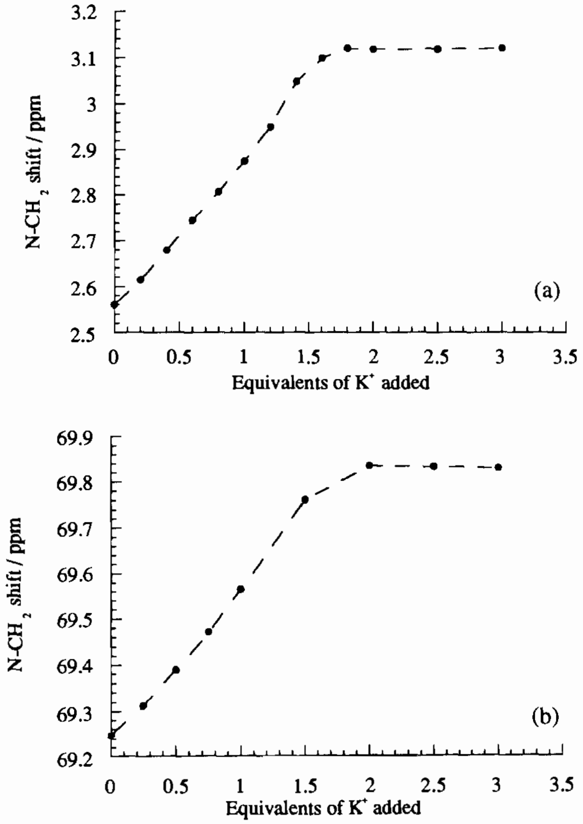

Fig. 3. Examples of ^{1}H and ^{13}C NMR titration curves for **6**: (a) ^{1}H NMR with Mg^{2+}; (b) ^{13}C NMR with K^+.

3.2. Coordination studies

The coordination chemistry of **4** and **5** has been reported previously [19]. ^{1}H and ^{13}C NMR Group 1 and 2 metal cation titration experiments were carried out with ligands **6** and **7** in deuterated acetonitrile solution. The addition of stoichiometric equivalents of Na^+, K^+, Mg^{2+} and Ba^{2+} cations caused significant perturbations of both ligands' respective NMR spectra. For example, Fig. 2 shows changes of the ^{1}H NMR spectrum of **6** upon addition of Mg^{2+} cations. The resulting titration curves (Fig. 3) suggest **6** forms 2:1 metal:ligand complexes with all the alkali metal cations, in which one metal cation is coordinated in each aza-18-crown-6 moiety.

With **7**, 2:1 metal:ligand complexes are produced with Na^+ and Mg^{2+} and 1:1 intramolecular sandwich complexes formed with the larger cations K^+ and Ba^{2+}.

Solid state orange crystalline complexes of **6** with K^+ and Ba^{2+} cations were successfully isolated (see Section 2) and crystals of the K^+ complex suitable for X-ray structure determination grown from a CH_2Cl_2/methanol solvent mixture. The structure (Fig. 4) shows the iron atom occupying a crystallographic centre of symmetry, thus the two cyclopentadienes are staggered. The two 18-membered crown rings are on opposite sides of the molecule and have the approximate D_{3d}

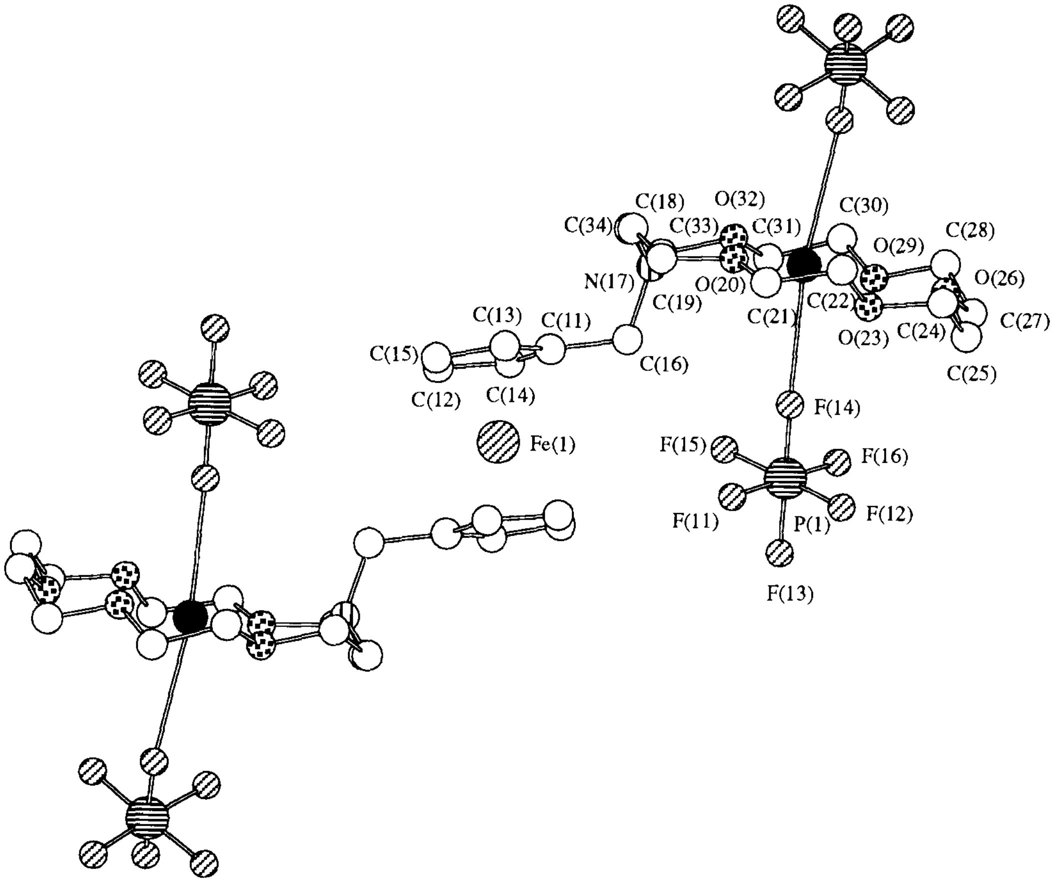

Fig. 4. Structure of $[\mathbf{6}\cdot 2K^+](PF_6^-)_2$.

Table 5
Electrochemical data for **6** and **7**

Cation	$\Delta E_{1/2}$ (mV)	
	6	**7**
Na^+	95	90
K^+	105	60
Ba^{2+}	150	
Mg^{2+}	385	200

Data were obtained in acetonitrile solution containing 0.2 M $Bu^n{}_4NBF_4$ as supporting electrolyte. Solutions were $\sim 3\times 10^{-3}$ M and potentials were determined with reference to Ag^+/Ag. The metal cation solutions were prepared from their perchlorate salts (except $K^+PF_6^-$) and the potentials quoted above were produced by addition of an excess of each cation.

conformation with all C–C–O–C and C–C–N–C torsion angles *trans* and O–C–C–O and N–C–C–O alternatively $+g$ and $-g$. The potassium cations are located in the centre of the rings with K–O distances varying from 2.744(6) to 2.767(6) Å and a K–N distance of 2.910(6) Å. These six donor atoms form an equatorial plane around the metal. In addition the potassium is bonded to two fluorine atoms of PF_6^- groups in axial positions at 2.843(10) and 2.844(10) Å.

3.3. Electrochemical studies

The electrochemical properties of **6** and **7** were initially investigated using cyclic voltammetry in acetonitrile solution with $(Bu^n)_4NBF_4$ as the supporting electrolyte. Each compound exhibited a reversible one-electron oxidation wave typical of a substituted ferrocene derivative (Table 5).

Cyclic voltammograms were also recorded after progressively adding stoichiometric equivalents of Na^+, K^+, Mg^{2+} or Ba^{2+} cations to the electrochemical solutions of **6** and **7**. Significant one-wave anodic shifts were observed with all metal cations. For example, Fig. 5 illustrates the anodic redox potential perturbations of the CV oxidation wave of **6** on addition of excess amounts of Na^+, K^+, Mg^{2+} and Ba^{2+} cations. The electrochemical Group 1 and 2 metal cation recognition results are summarised in Table 5. In agreement with electrochemical recognition studies of ferrocenyl benzo-crown ether ligand systems [8,9], the magnitude of the anodic shift (ΔE) is dependent upon the polarising power of the particular metal cationic guest. The magnesium dication produces the largest perturbation of 385 mV with **6** as it possesses, in comparison with the other metal cations, the greatest charge to metal cation radius ratio. It is noteworthy however that although

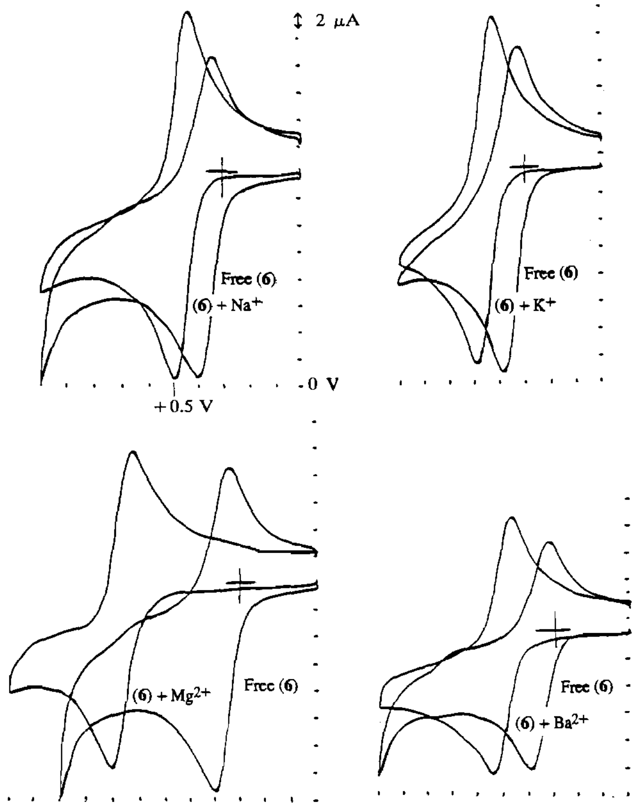

Fig. 5. Cyclic voltammograms of 6 + Group 1 and 2 metal cations in CH_3CN. In each case $x = 100$ mV cm^{-1}, $y = 2$ μA cm^{-1}, scan rate = 100 mV s^{-1}.

ligand 7 and Na^+ cations produces the expected larger anodic shift perturbation ($\Delta E = 90$ mV) over that of K^+ cations ($\Delta E = 60$ mV), surprisingly the reverse trend is observed with redox ionophore 6 (i.e. $\Delta E(Na^+) = 95$ mV versus $\Delta E(K^+) = 105$ mV).

Of particular relevance to amperometric chemical sensor technology were the novel results of electrochemical competition experiments with **6**. When an equimolar mixture of Na^+, K^+, Mg^{2+} and Ba^{2+} cations was added to an acetonitrile electrochemical solution of **6** the respective ferrocene–ferrocenium redox couple shifted anodically by an amount approximately the same as that induced by the Ba^{2+} alone. This observation implies that although the largest perturbation occurs with the cation possessing the greatest charge to radius ratio, the greater selectivity is achieved when the cation size is more appropriate to that of the crown ether ring. The 18-crown-6 ring has a diameter of approx. 5.5 Å compared with the radius of Ba^{2+} (1.35 Å) and Mg^{2+} (0.65 Å). In addition other factors, such as solvation, may come into play. The larger, less solvated cations are more competitive in the complexation process and may help to explain the greater affinity of **6** for Ba^{2+} over Mg^{2+}. This result suggests **6** is a first generation prototype barium cation selective amperometric sensor, capable of detecting Ba^{2+} in the presence of alkali metal cations Na^+, K^+ and Mg^{2+}.

4. Conclusions

New bis(aza-crown ethers) **6** and **7** have been synthesised in which a ferrocene redox centre bridges the two respective aza-crown ether moieties, linked via methylene covalent bonds. Coordination chemical investigations revealed both ligands complex Group 1 and 2 metal cations. Electrochemical studies have demonstrated that these redox-active ionophores electrochemically recognise Na^+, K^+, Mg^{2+} and Ba^{2+} guest cations via initial aza-crown ether cation complexation and electrostatic 'through space' perturbation of the respective ferrocene–ferrocenium redox couple, producing a shift to more positive potentials. The charge to radius ratio or polarising power of the guest metal cation is of paramount importance in determining the magnitude of anodic shift in redox potential of the ferrocenyl redox centre. Electrochemical recognition competition experiments in acetonitrile suggest **6** exhibits a degree of selectivity for the Ba^{2+} cation over the other alkali metal cations.

Acknowledgements

We thank the S.E.R.C. for a studentship to A.J.P. and for the use of the mass spectrometry service at University College, Swansea.

References

[1] (a) P.D. Beer, *Chem. Soc. Rev., 18* (1989) 409; (b) *Adv. Inorg. Chem., 39* (1992) 79.
[2] N. Al-Odaidi, P.D. Beer, J.P. Bright, C.J. Jones, J.A. McCleverty and S.S. Salam, *J. Chem. Soc., Chem. Commun.*, (1986) 239.
[3] R.E. Wolfjun and S.R. Cooper, *J. Am. Chem. Soc., 106* (1984) 4646.
[4] L. Echegoyen, D.A. Gustowski, V.J. Gatto and G.W. Gokel, *J. Chem. Soc., Chem. Commun.*, (1986) 220.
[5] D.A. Gustowski, L. Echegoyen, D.M. Goli, A. Kaifer, R.A. Schultz and G.W. Gokel, *J. Am. Chem. Soc., 106* (1984) 1633.
[6] P.D. Beer, *J. Chem. Soc., Chem. Commun.*, (1985) 1115.
[7] T. Saji, *Chem. Lett.*, (1986) 275.
[8] P.D. Beer, C. Blackburn, J.F. McAleer and H. Sikanyika, *Inorg. Chem., 29* (1990) 378.
[9] P.D. Beer, H. Sikanyika, C. Blackburn, J.F. McAleer and M.G.B. Drew, *J. Chem. Soc., Dalton Trans.*, (1990) 3295.
[10] C.D. Hall, N.W. Sharpe, I.P. Danks and Y.P. Sang, *J. Chem. Soc., Chem. Commun.*, (1989) 419.
[11] E. Fu, M.L.H. Green, V.J. Lowe and S.R. Marder, *J. Organomet. Chem., 341* (1988) C39.
[12] F.C.J.M. van Veggel, S. Harkema, M. Bus, W. Verboom, G.K. Klein, G. Woolthius and D.N. Reinhoudt, *J. Org. Chem., 54* (1989) 2351.
[13] N.D. Lowe and C.D. Garner, *J. Chem. Soc., Dalton Trans.*, (1993) 2197.
[14] T. Jørgensen, T.K. Hansen and J. Becher, *Chem. Soc. Rev., 23* (1994) 41.
[15] P.D. Beer, D.B. Crowe, M. Ogden, M.G.B. Drew and B. Main, *J. Chem. Soc., Dalton Trans.*, (1993) 2107.

[16] P.D. Beer, D. Hesek, J. Hodacova and S.E. Stokes, *J. Chem. Soc., Chem. Commun.*, (1992) 270.

[17] P.D. Beer, C.A.P. Dickson, N. Fletcher, A.J. Goulden, A. Grieve, J. Hodacova and T. Wear, *J. Chem. Soc., Chem. Commun.*, (1993) 828.

[18] (a) J.C. Medina, T.T. Goodnow, M.T. Rogers, J.L. Atwood, B.C. Lynn, A.E. Kaifer and G.W. Gokel, *J. Am. Chem. Soc., 114* (1992) 10583; (b) P.D. Beer, Z. Cheng, M.G.B. Drew, J. Kingston, M. Ogden and P. Spencer, *J. Chem. Soc., Chem. Commun.*, (1993) 1046.

[19] P.D. Beer, A.D. Keefe, H. Sikanyika, C. Blackburn and J.F. McAleer, *J. Chem. Soc., Dalton Trans.*, (1990) 3289.

[20] H.J. Lorkowski, R. Pannier and A. Wende, *J. Prakt. Chem., 35* (1967) 149.

[21] M.R. Johnson, I.O. Sutherland and R.F. Newton, *J. Chem. Soc., Perkin Trans. 1*, (1979) 357.

[22] W. Kabsch, *J. Appl. Crystallogr., 21* (1989) 916.

[23] G.M. Sheldrick, *SHELX 86 Program for Structure Solution*, University of Groningen, Germany, 1986.

[24] G.M. Sheldrick, *SHELX 1 Program for Structure Refinement*, University of Groningen, Germany, 1993.